

## Supplementary Information

# Precisely Tailored LaFeO<sub>3</sub> Dendrites using Urea and Piperazine Hexahydrate for Highly Sensitive, Selective and Trace Level Detection of Acetone

*K Palani Thiruppathi<sup>a,b</sup> and Devaraj Nataraj<sup>a,b,c\*</sup>*

<sup>a</sup> Physics Division, DRDO – BU Centre for Life Sciences, Bharathiar University Campus, Coimbatore – 641 046, India.

<sup>b</sup> Quantum Materials & Devices Laboratory, Department of Physics, Bharathiar University, Coimbatore – 641 046, India.

<sup>c</sup> UGC-CPEPA Centre for Advanced Studies in Physics for the development of Solar Energy Materials and Devices, Department of Physics, Bharathiar University, Coimbatore – 641 046, India.

\*Corresponding Author E-mail: de.natraj2011@gmail.com

**Table S1.** Detailed reactant concentrations and corresponding outcomes

S. No	Sample code	Piperazine hexahydrate mM [mg]	Urea mM [mg]	Before/ After pH	Crystalline Phase	Morphology
1	U9	0	9 (540.54)	2.67/9.30	LaFeO <sub>3</sub>	Irregular Particle with Aggregation
2	U9P3	3 (582.69)	9 (540.54)	6.74/9.35	La(OH) <sub>3</sub> , LaFeO <sub>3</sub>	Parallelogram and Irregular Structures
3	U9P6	6 (1165.38)	9 (540.54)	9.49/9.56	LaFeO <sub>3</sub>	Dendritic Growth Initiation
4	U9P9	9 (1748.07)	9 (540.54)	9.54/9.60	LaFeO <sub>3</sub>	Early - Stage Dendrites
5	U9P12	12 (2330.76)	9 (540.54)	9.88/9.92	LaFeO <sub>3</sub>	Mid - Stage Dendrites
6*	U9P15	15 (2913.45)	9 (540.54)	9.90/9.90	LaFeO <sub>3</sub>	Fully Grown Dendrites
7	U9P18	18 (3496.14)	9 (540.54)	10.01/10.03	LaFeO <sub>3</sub>	Fully Grown Dendrites
8	U9P21	21 (4078.83)	9 (540.54)	10.10/10.12	LaFeO <sub>3</sub>	Fully Grown Dendrites
9	P15	15 (2913.45)	0	9.88/9.90	La <sub>2</sub> O <sub>3</sub> , Fe <sub>2</sub> O <sub>3</sub> , LaFeO <sub>3</sub>	Matured Dendrites

**Note :** (1) Stoichiometric ratio of 1 mM La(NO<sub>3</sub>)<sub>3</sub> . xH<sub>2</sub>O and 1 mM Fe(NO<sub>3</sub>)<sub>3</sub> . 9H<sub>2</sub>O were used for all reactions.

(2) The reaction temperature was kept at 180 °C for 24 h.

(3) The final products were dried at 110 °C for 1 h and calcinated at 900 °C for 3 h.

(4) \* represents the optimized final reactant concentration.

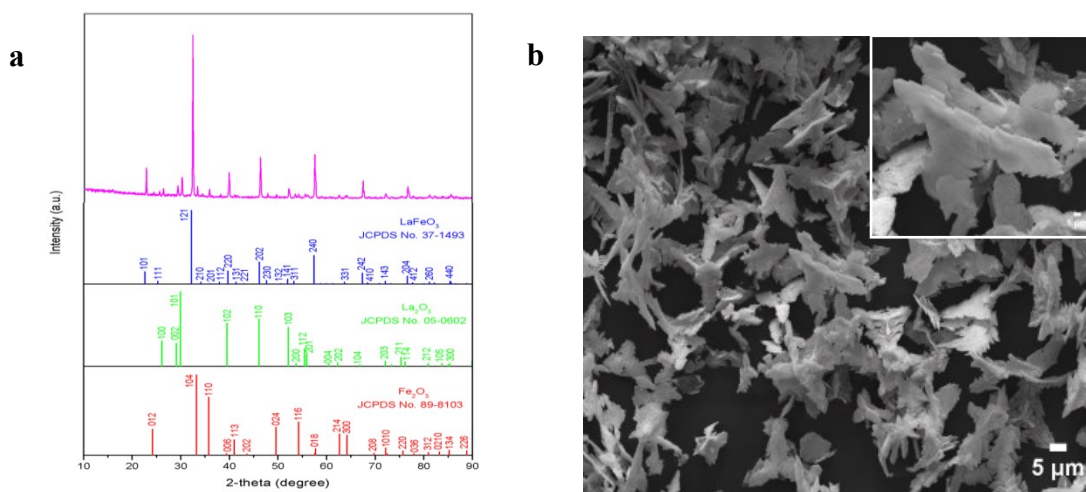


**Fig. S1** a) XRD pattern and b) SEM images of 15 mM piperazine hexahydrate (P15) assisted LaFeO<sub>3</sub> dendrites formation process.

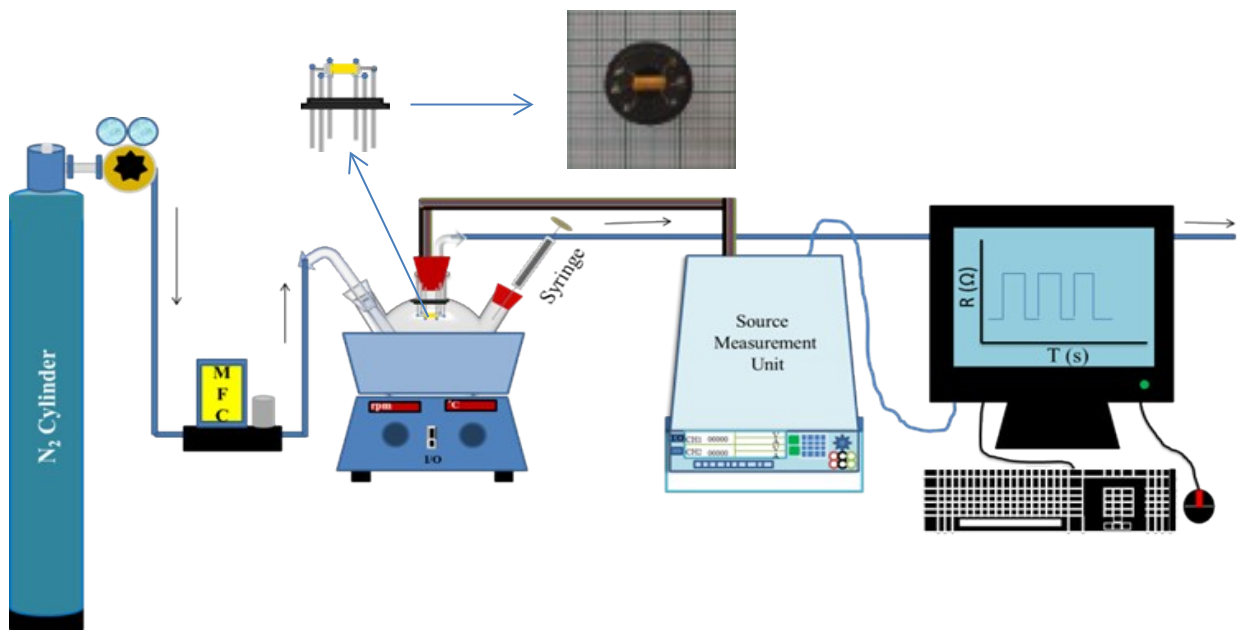


**Fig. S2** Schematic illustration of custom made vapor sensing arrangement and photograph of fabricated sensing device.

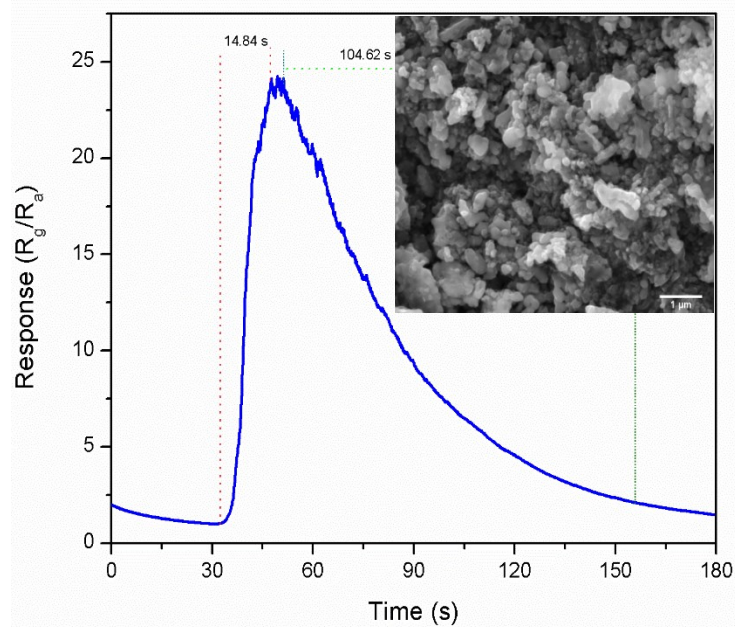


**Fig. S3** 1 ppm acetone sensing response using irregular LaFeO<sub>3</sub> particles at 100 °C device and chamber temperatures. (Inset : SEM image of irregular LaFeO<sub>3</sub> particles)

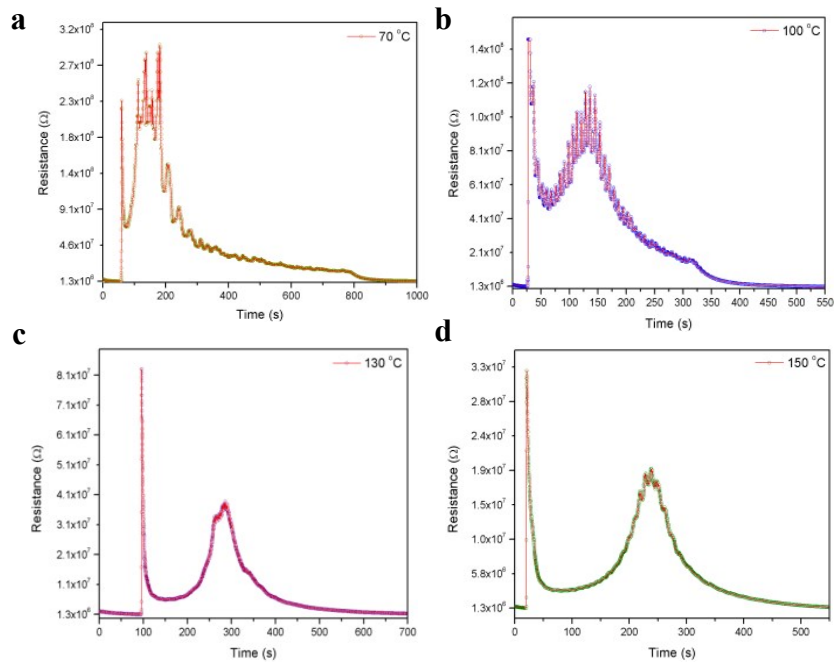


**Fig. S4** 10 ppm pure acetone sensing response using LaFeO<sub>3</sub> dendrites (U9P15) at a) 70 °C, b) 100 °C, c) 130 °C and d) 150 °C chamber temperatures with 100 °C device temperature.

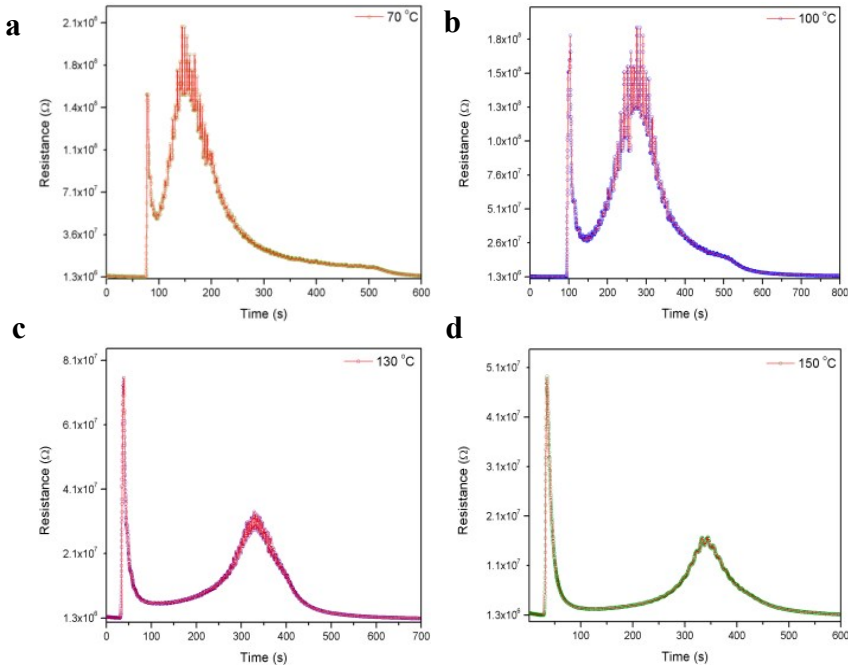


**Fig. S5** 10 ppm pure ethanol sensing response using LaFeO<sub>3</sub> dendrites (U9P15) at a) 70 °C, b) 100 °C, c) 130 °C and d) 150 °C chamber temperatures with 100 °C device temperature.

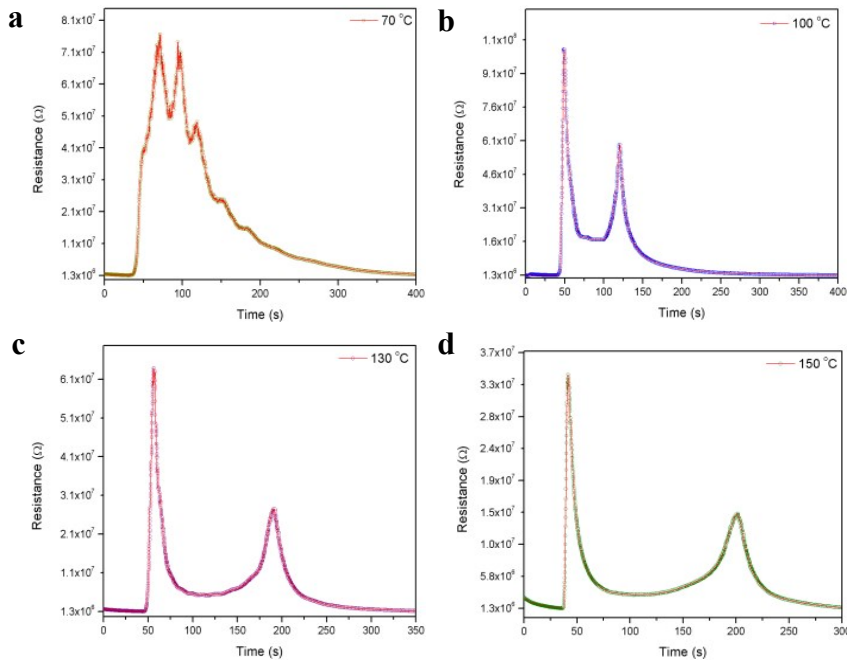


**Fig. S6** 10 ppm (37 - 41%) formaldehyde sensing response using LaFeO<sub>3</sub> dendrites (U9P15) at a) 70 °C, b) 100 °C, c) 130 °C and d) 150 °C chamber temperatures with 100 °C device temperature.

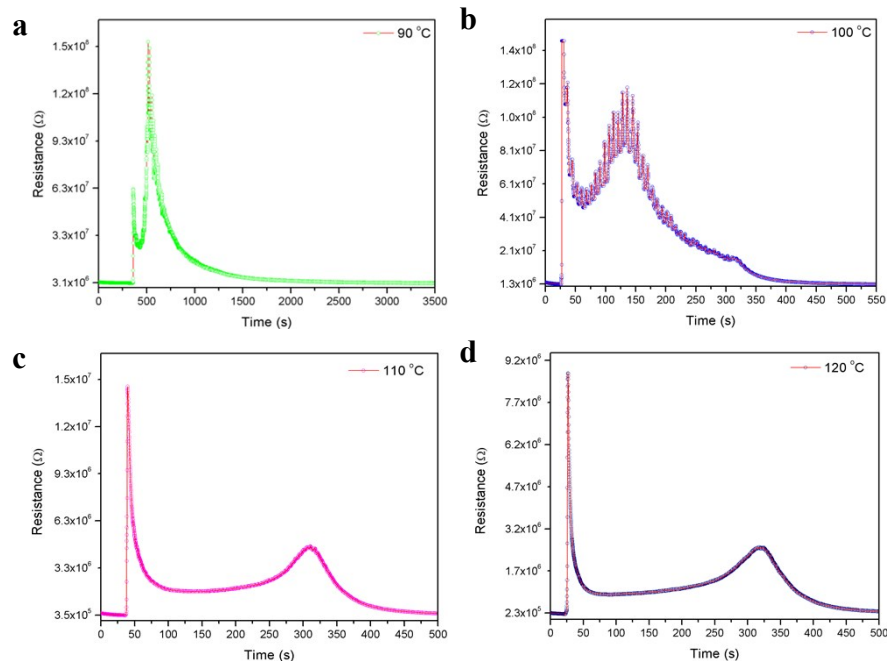


**Fig. S7** 10 ppm pure acetone sensing response using LaFeO<sub>3</sub> dendrites (U9P15) at a) 90 °C, b) 100 °C, c) 110 °C and d) 120 °C device temperatures with 100 °C chamber temperature.

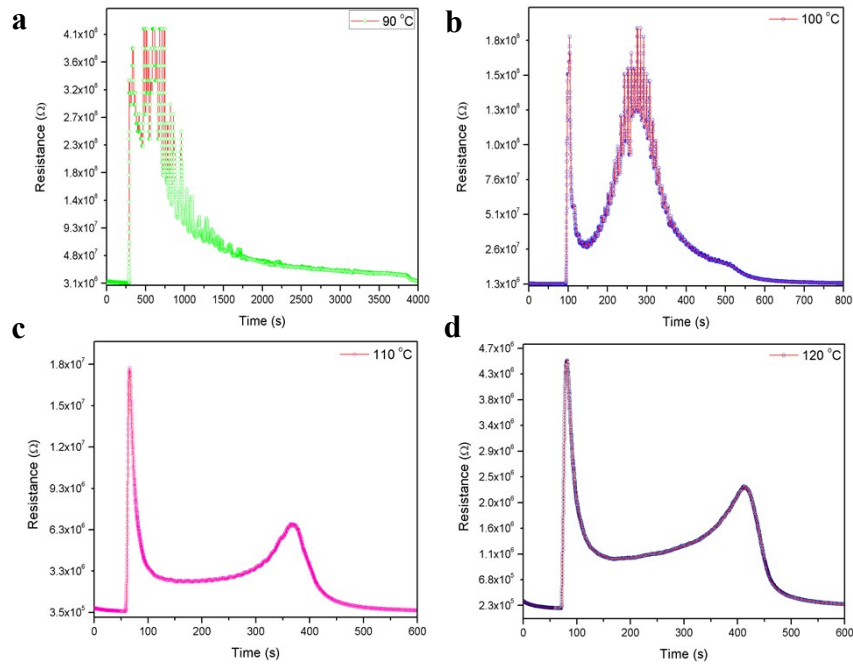


**Fig. S8** 10 ppm pure ethanol sensing response using LaFeO<sub>3</sub> dendrites (U9P15) at a) 90 °C, b) 100 °C, c) 110 °C and d) 120 °C device temperatures with 100 °C chamber temperature.

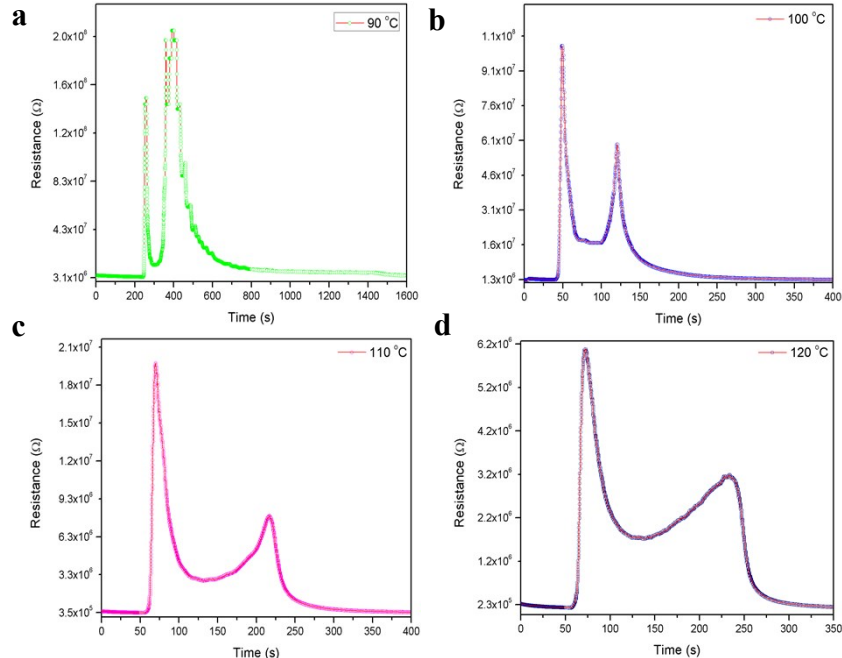


**Fig. S9** 10 ppm (37 - 41%) formaldehyde sensing response using LaFeO<sub>3</sub> dendrites (U9P15) at a) 90 °C, b) 100 °C, c) 110 °C and d) 120 °C device temperatures with 100 °C chamber temperature.

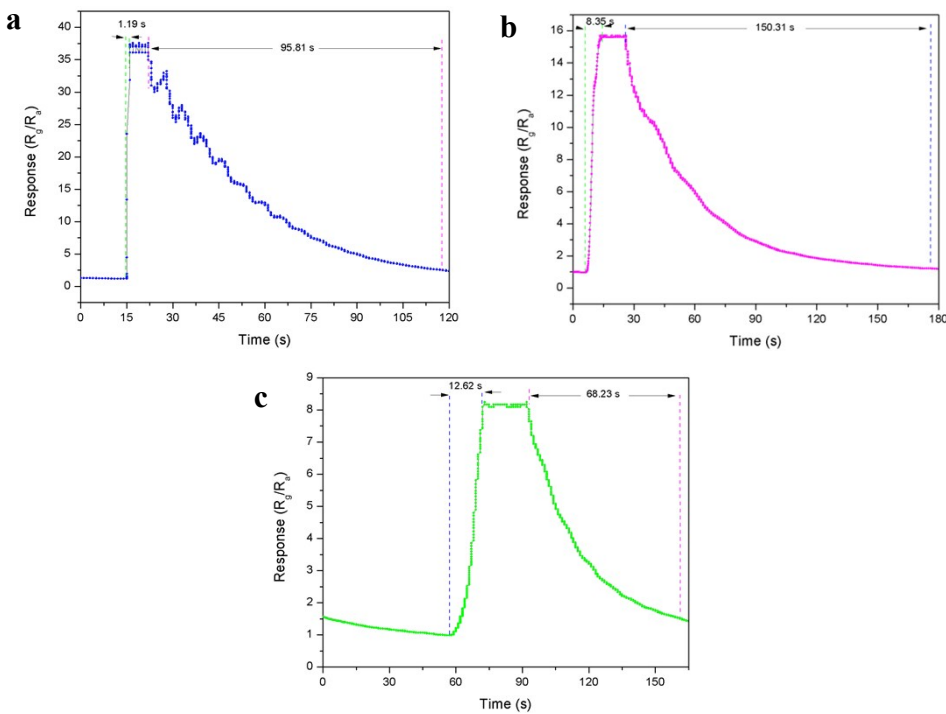


**Fig. S10** Response / recovery time of 1 ppm (a) acetone, (b) ethanol and (c) formaldehyde at 100 °C device and chamber temperatures.

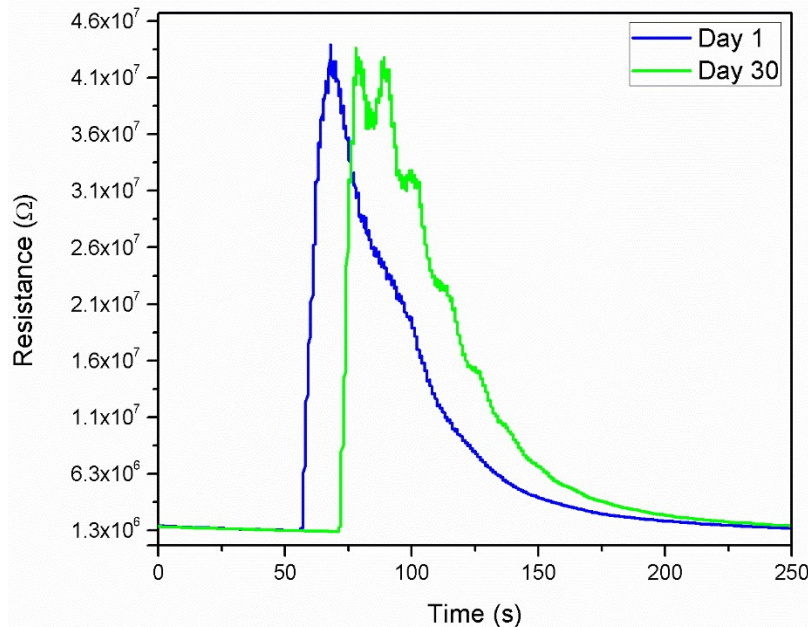


**Fig. S11** Comparison of 1 ppm acetone sensing response for day 1 and day 30 using LaFeO<sub>3</sub> dendrites at 100 °C device and chamber temperatures.

**Table S2.** Comparison of recently reported acetone sensors with the present LaFeO<sub>3</sub> dendrites based device.

Sensing Materials	Concentration [ppm]	Sensing Response $S = R_g/R_a$ or $R_a/R_g$	T <sub>res/rec</sub> [s]	Lowest Detection [ppm]	Operating Temperature [°C]	Ref
<b>3 mol% Co-doped Spongy-like In<sub>2</sub>O<sub>3</sub></b>	100	32.8	1.14/37.5	5	240	1
<b>Porous WO<sub>3</sub> Nanofibers</b>	12.5	1.79	33/42	1.8	350	2
<b>3 wt% Pd:SmFe<sub>0.9</sub>Mg<sub>0.1</sub>O<sub>3</sub> Nanocrystalline Powders</b>	0.5	7.16	32/8	0.01	220	3
<b>Co<sub>3</sub>O<sub>4</sub> Core–Shell</b>	200	13	4/8	10	190	4
<b>PdO–NiO/NiCo<sub>2</sub>O<sub>4</sub> Truncated Nanocages</b>	100	6.7	19/28	10	210	5
<b>Porous Tube-like Au/ZnO</b>	100	280	2/92	1	190	6
<b>0.070 wt% Pt-Functionalized CS-Pt@SnO<sub>2</sub> Nanofiber</b>	1	37.9	12/44	0.1	350	7
<b>Bi<sub>2</sub>O<sub>3</sub> Nanostructures</b>	100	41%	315/152	10	27	8
<b>Hollow NiFe<sub>2</sub>O<sub>4</sub> Microspindles</b>	200	52.8	14.2/>100	5	120	9
<b>MWCNTs/Co<sub>3</sub>O<sub>4</sub> Octahedron</b>	100	5.1	-	10	120	10
<b>Multilayer-assembled ZnO Nanoplates</b>	100	21.56	9/51	0.25	230	11
<b>Concave ZnFe<sub>2</sub>O<sub>4</sub> Hollow Octahedral Nanocages</b>	100	35.5	-	5	120	12
<b>PdO–Co<sub>3</sub>O<sub>4</sub> Hollow Nanocages</b>	5	2.51	-	0.4	350	13
<b>PdO–ZnO Composite on Hollow SnO<sub>2</sub> Nanotubes</b>	1	5.06	16/36	0.1	400	14
<b>PtO<sub>2</sub> - SnO<sub>2</sub> Multichannel Nanofibers</b>	5	194.15	<12/-	0.4	400	15
<b>γ-Fe<sub>2</sub>O<sub>3</sub> Microrod</b>	100	125.5	0.9/15	10	220	16
<b>LaFeO<sub>3</sub> Dendrites</b>	<b>1</b>	<b>37.63</b>	<b>1.19/ 95.81</b>	<b>0.01</b>	<b>100</b>	<b>This work</b>

## References

- 1 X. Zhang, D. Song, Q. Liu, R. Chen, J. Liu, H. Zhang, J. Yu, P. Liu and J. Wang, *CrystEngComm*, 2019, **21**, 1876.
- 2 M. Imran, S. S. A. A. H. Rashi, Y. M. Sabri, N. Motta, T. Tesfamichael, P. M. Sonar and M. Shafiei, *J. Mater. Chem. C*, 2019, **7**, 2961.
- 3 H. Zhang, H. Qin, P. Zhang, and J. Hu, *ACS Appl. Mater. Interfaces*, 2018, **10**, 15558.
- 4 R. Zhang, T. Zhou, L. Wang, and T. Zhang, *ACS Appl. Mater. Interfaces*, 2018, **10**, 9765.
- 5 T. Zhou, X. Liu, R. Zhang, Y. Wang, and T. Zhang, *ACS Appl. Mater. Interfaces*, 2018, **10**, 37242.
- 6 H. Fu, X. Wang, P. Wang, Z. Wang, H. Ren and C. Wang, *Dalton Trans.*, 2018, **47**, 9014.
- 7 Y. J. Jeong, W. Koo, J. Jang, D. Kim, H. Cho and I. Kim, *Nanoscale*, 2018, **10**, 13713.
- 8 P. Shinde, B. Ghule, N. M. Shinde, Q. X. Xia, S. Shaikh, A. V. Sarode, R. S. Mane and K. H. Kim, *New J. Chem.*, 2018, **42**, 12530.
- 9 X. Song, F. Sun, S. Dai, X. Lin, K. Sun and X. Wang, *Inorg. Chem. Front.*, 2018, **5**, 1107.
- 10 R. Zhang, M. Zhang, T. Zhou and T. Zhang, *Inorg. Chem. Front.*, 2018, **5**, 2563.
- 11 M. Wang, Z. Shen, Y. Chen, Y. Zhang and H. Ji, *CrystEngComm*, 2017, **19**, 6711.
- 12 X. Z. Song, Y. L. Meng, Z. Tan, L. Qiao, T. Huang, and X. F. Wang, *Inorg. Chem.* 2017, **56**, 13646.
- 13 W. T. Koo, S. Yu, S. J. Choi, J. S. Jang, J. Y. Cheong, and I. D. Kim, *ACS Appl. Mater. Interfaces*, 2017, **9**, 8201.
- 14 W. T. Koo, J. S. Jang, S. J. Choi, H. J. Cho, and I. D. Kim, *ACS Appl. Mater. Interfaces* 2017, **9**, 18069.
- 15 Y. J. Jeong, W. T. Koo, J. S. Jang, D. H. Kim, M. H. Kim, and I. D. Kim, *ACS Appl. Mater. Interfaces*, 2018, **10**, 2016.
- 16 Z. Song, H. Chen, S. Bao, Z. Xie, Q. Kuang and L. Zheng, *J. Mater. Chem. A*, 2020, **8**, 3754.